

---

***Donald Kaplan's Legacy: Influencing Teaching and Research***  
*Guest edited by D. A. DeMason and A. M. Hirsch*

## **Do Fibonacci numbers reveal the involvement of geometrical imperatives or biological interactions in phyllotaxis?**

TODD J. COOKE\*

*Department of Cell Biology and Molecular Genetics, University of Maryland, College Park, MD 20742, USA*

*Received December 2004; accepted for publication April 2005*

---

Complex biological patterns are often governed by simple mathematical rules. A favourite botanical example is the apparent relationship between phyllotaxis (i.e. the arrangements of leaf homologues such as foliage leaves and floral organs on shoot axes) and the intriguing Fibonacci number sequence (1, 2, 3, 5, 8, 13 . . .). It is frequently alleged that leaf primordia adopt Fibonacci-related patterns in response to a universal geometrical imperative for optimal packing that is supposedly inherent in most animate and inanimate structures. This paper reviews the fundamental properties of number sequences, and discusses the under-appreciated limitations of the Fibonacci sequence for describing phyllotactic patterns. The evidence presented here shows that phyllotactic whorls of leaf homologues are not positioned in Fibonacci patterns. Insofar as developmental transitions in spiral phyllotaxis follow discernible Fibonacci formulae, phyllotactic spirals are therefore interpreted as being arranged in genuine Fibonacci patterns. Nonetheless, a simple modelling exercise argues that the most common spiral phyllotaxes do not exhibit optimal packing. Instead, the consensus starting to emerge from different subdisciplines in the phyllotaxis literature supports the alternative perspective that phyllotactic patterns arise from local inhibitory interactions among the existing primordia already positioned at the shoot apex, as opposed to the imposition of a global imperative of optimal packing. © 2006 The Linnean Society of London, *Botanical Journal of the Linnean Society*, 2006, **150**, 3–24.

**ADDITIONAL KEYWORDS:** auxin – golden ratio – number sequence – optimal packing – spiral phyllotaxis – whorled phyllotaxis.

---

### INTRODUCTION

Western philosophy has two major complementary intellectual traditions: (1) Platonic idealism, in which an overarching theory is used to integrate existing observations and to predict new observations, and (2) Aristotelian empiricism, in which individual observations are used to construct a unifying theory. Phyllotaxis, which is broadly defined as the arrangement of leaf homologues (i.e. lateral determinate organs) on shoot axes, has perhaps attracted wider attention than most other botanical subjects in part because it

appeals to the proponents and practitioners of both traditions. Those scientists interested in theoretical approaches, including idealistic morphologists and theoretical biophysicists such as Goethe, Braun, Thompson and Green, have attempted to construct an appealing synthetic theory for explaining phyllotactic patterning, and then search for compelling botanical examples to support that theory. By contrast, those favouring empirical approaches, including comparative morphologists and molecular geneticists such as Hofmeister, Kaplan, Meyerowitz and Kuhlemeier, have studied phyllotactic patterns in a range of different plants or genetic variants in the hope that this comparative approach might reveal fundamental

---

\*Corresponding Author. E-mail: tc23@umail.umd.edu

principles or underlying mechanisms. What has the potential to tie these disparate approaches together is the widespread recognition that phyllotaxis displays some truly remarkable and quite seductive mathematical properties. Moreover, judging from the popular literature, the mathematics of phyllotaxis has allowed this problem to transcend specialized scientific interests so that it has also captured the imagination of the educated public.

It is often asserted that geometrical patterns in biological structures are likely to result from simple physical processes, such as surface tension, mechanical stress and fluid dynamics, that are intrinsic to matter itself (e.g. Thompson, 1942; Ball, 1999; Stewart, 2001). According to this perspective, biological pattern is seen as the unavoidable consequence of what might be called geometrical imperatives that operate on both inanimate and animate structures. No other phenomenon in plant morphology seems a more likely candidate for arising from the action of a geometrical imperative than does phyllotaxis. In seed plants, despite an infinite number of conceivable arrangements, the leaves are arranged in two basic patterns: spiral patterns composed of one leaf per node, and whorled patterns composed of two or more leaves per node. It is repeatedly claimed that these patterns can be described with reference to a simple, apparently universal and incredibly intriguing number sequence known as the Fibonacci sequence.

As the expression says, fools rush in where angels fear to tread, and thus my colleague Wanda Kelly and I are proceeding in accordance with our naïve belief that the disciplines mentioned above have already made the crucial discoveries for establishing the conceptual framework needed to solve phyllotaxis as a scientific problem. In our opinion, it has been the failure of each discipline to take the discoveries from the other disciplines into account that has prevented the botanical community as a whole from recognizing this great achievement. We are currently making selected observations designed to integrate those discoveries from various disciplines into a coherent framework (for our first contribution, see Kelly & Cooke, 2003). The present paper attempts to perform a clear-sighted analysis of the Fibonacci sequence and its relationship to plant phyllotaxis in an effort to separate botanical essence from the Pythagorean mysticism plaguing many scientific and popular expositions. In particular, the objectives of this paper are: (1) to describe the fundamental properties of number sequences; (2) to interpret the Fibonacci number sequence with respect to these properties in order to illustrate its inherent limitations for describing certain phyllotactic arrangements; and (3) to evaluate whether the phyllotaxes exhibiting genuine Fibonacci-based patterns arise from the universal geometrical imperative of optimal

packing or whether they are generated as the consequence of the underlying biological interactions specifying leaf position.

## FUNDAMENTAL PROPERTIES OF FIBONACCI SEQUENCES

### A PRIMER ON NUMBER SEQUENCES

This section provides an elementary description of the critical features of number sequences. A number sequence is defined as any set of numbers that are arranged in a prescribed order. Of particular interest are certain sequences known as recursive sequences, where each term is defined as a function of the preceding term(s). A class of related recursive number sequences is fundamentally defined by the mathematical *formula* or rule used to generate each sequence in that class. For instance, the number sequence

$$1, 2, 4, 8, 16, 32, 64, 128, 256, 512, \dots$$

is generated by doubling the preceding term to produce the succeeding term. Its formula can be symbolized as

$$2x_{n-1} = x_n,$$

where  $x_{n-1}$  and  $x_n$  represent the values of the preceding term ( $n-1$ ) and succeeding term ( $n$ ), respectively. Using the same formula, it is possible to generate another number sequence in this class as

$$3, 6, 12, 24, 48, 96, 192, 384, 768, \dots$$

It is seen from these two examples is that one feature capable of distinguishing between two particular sequences within a class is the *initial term* (or initial terms in those classes where the formula acts on more than one preceding term to generate the succeeding term). Indeed, the formula and the initial term(s) are entirely sufficient together to define a unique recursive sequence (Vorobyov, 1963; Koshy, 2001).

Another feature that can help to characterize a number sequence is its *limit*, which represents the number that is ultimately approached by a sequence composed of many numbers. Many sequences such as the two listed above diverge without any finite limit so that they can be said to reach a limit of infinity. Far more interesting are those sequences that converge on a specific number, such as

$$1, \frac{1}{2}, \frac{1}{4}, \frac{1}{8}, \frac{1}{16}, \frac{1}{32}, \frac{1}{64}, \dots$$

which is generated by the formula  $x_{n-1} = 2x_n$ .

Of course, the limit for this sequence is zero. It is worth noting for future reference that the limit of a converging sequence may have unique properties that are not shared by the actual numbers in that sequence. In this particular example, all the numbers, no matter how infinitesimally small, in this sequence



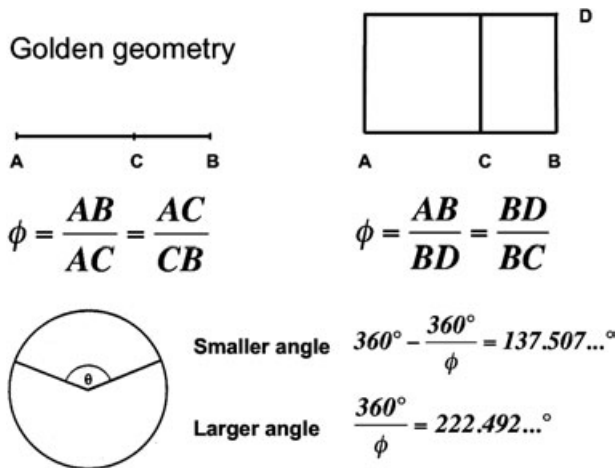


**Figure 2.** Several examples of golden geometry derived from the golden ratio ( $\phi$ ), which was first recognized as the division of a line such that the ratio of the line to the larger segment is equal to the ratio of the larger segment to smaller segment.

Golden Ratio (for informative essays, see Huntley, 1970; Dunlap, 1997; Kappraff, 2002; Livio, 2002). The reader is referred to the Appendix for additional information about the fascinating numerical properties of  $\phi$ .

The golden ratio derived from the subdivision of a line leads to many other geometrical relationships that comprise what might be called 'golden geometry' (Coxeter, 1953; Vorobyov, 1963; Hoggatt, 1969; Huntley, 1970; Vajda, 1989; Koshy, 2001; Kappraff, 2002; Livio, 2002). For instance, a golden rectangle can be drawn from the golden segment (ACB) such that the ratio of the longer side (AB) over the shorter side (BD) is also equal to  $\phi$  (Fig. 2). If the largest possible square is drawn within the golden rectangle, then the remaining rectangle must have the same proportions as the original rectangle meaning that the aspect ratio of the new longer side (BD) over the new shorter side (BC) is once again equal to  $\phi$ . In terms of an equation,

$$\phi = \frac{AB}{BD} = \frac{BD}{BC}.$$

The golden rectangle can thus be said to exhibit the property of self-regeneration in that a larger golden rectangle can be subdivided to generate a square and a smaller golden rectangle. This subdivision process can be continuing *ad infinitum*, with the result that each subdivision results in an even smaller rectangle with an aspect ratio of  $\phi$ . This process of repeated subdivisions leaves a never-reachable point of free space, which is referentially known as the 'Eye of God', near the centre of the golden rectangle. The golden rectangle is the only rectangle with the property whereby the cutting off of the largest possible square produces a

smaller rectangle with an identical shape as the original rectangle.

Similarly, it is possible to divide a circle into two golden angles, which exhibit the following relationships (Fig. 2):

$$\phi = \frac{360^\circ}{\theta_1} = \frac{\theta_1}{\theta_s},$$

where  $\theta_1$  and  $\theta_s$  represent the larger and smaller golden angles of the circle, respectively. Rearranging this equation to solve it for the angles,

$$\theta_l = \frac{360^\circ}{\phi} = 222.492\dots^\circ$$

and

$$\theta_s = \frac{\theta_l}{\phi} = 137.507\dots^\circ$$

$\theta_s$  is the so-called golden or ideal angle often proposed to represent the optimal displacement of leaf primordia on shoot apices, as is examined in a later section. An alternative method for calculating the ideal angle involves the limit of the reciprocal primary fractional series starting with the initial terms of 1/3, 2/5 and 3/8. This limit is equal to  $\phi^{-2}$ , as is shown in Appendix Table A2. Then

$$\theta_s = 360^\circ(\phi^{-2}) = 137.507\dots^\circ$$

#### UNDER-APPRECIATED MATHEMATICAL CONSTRAINTS ON THE APPLICATION OF FIBONACCI SEQUENCES TO BIOLOGICAL PHENOMENA

The Fibonacci literature has unbridled enthusiasm for identifying the putative involvement of the Fibonacci sequence in biological, and especially botanical, phenomena (e.g. Coxeter, 1953; Huntley, 1970; Garland, 1987; Koshy, 2001; Britton, 2003; Knott, 2004). It makes one almost forget that the Fibonacci sequence was first devised as the solution to a *hypothetical* mathematical problem about rabbit population growth. I believe that we botanists are well advised to express greater scepticism toward any alleged example of the botanical manifestation of the Fibonacci sequence. The following questions can be used to inform our thinking on this issue.

(1) Does an individual grouping of biological objects as a primary Fibonacci number provide compelling evidence for the underlying participation of the Fibonacci sequence? The numbers 2, 3 and 5 (and their multiples) are frequently alleged to disclose the involvement of the Fibonacci sequence in a given process because they are taken to represent unique Fibonacci numbers as opposed to other 'non-Fibonacci' numbers. It follows from this allegation that any

structure appearing in a group of 5, such as the digits on the human hand or the petals of a rose flower, can be interpreted as being a manifestation of the Fibonacci sequence. This argument is easily refuted by re-examining Figure 1. It is worth noting that the first six positive integers are either components or multiples of the primary Fibonacci sequence; thus, a small group must be composed of at least 7 units before it appears to be unrelated to the primary Fibonacci sequence. Furthermore, of the first 21 integers, 7 integers are included in the primary sequence and 12 integers are multiples of those 7 integers (Fig. 1). Two numbers, 8 and 21, are both components and multiples of the primary sequence. Thus, almost every small group of biological objects must unavoidably be quantified in terms of Fibonacci numbers. It might instead be argued that the only meaningful grouping of biological objects might be those groups of 7, 11, 17 or 19 that have no obvious relation to the primary Fibonacci sequence!

In fact, being a component of Fibonacci sequences is an intrinsic property of all positive integers. If we restrict our attention to only those Fibonacci sequences starting with an initial term of either 1 or 2, then 3 is a term in two non-redundant sequences, namely the primary and first accessory Fibonacci sequences (Fig. 1), whereas 4 is a part of three non-redundant sequences, namely the first accessory sequence plus two other sequences:

$$\begin{aligned} &1, 4, 5, 9, 14, \dots \\ &2, 4, 6, 10, 16, \dots \end{aligned}$$

All integers ( $n$ ) greater than 4 belong to at least four non-redundant Fibonacci sequences starting with the initial terms of 1 or 2 as follows:

$$\begin{aligned} &1, n, n+1, 2n+1, \dots \\ &1, n-1, n, 2n-1, \dots \\ &2, n, n+2, 2n+2, \dots \\ &2, n-2, n, 2n-2, \dots \end{aligned}$$

In addition, all odd integers 7 or above belong to at least one additional non-redundant sequence given as

$$1, \frac{1}{2}(n-1), \frac{1}{2}(n+1), n, \frac{1}{2}(3n+1), \dots$$

Similarly, all even integers 8 or above belong to at least one additional non-redundant sequence given as

$$2, \frac{1}{2}(n-2), \frac{1}{2}(n+2), n, \frac{1}{2}(3n+2), \dots$$

These considerations show that all positive integers can be considered as being Fibonacci numbers. It follows that a single number by itself does not allow us to discriminate between a genuine Fibonacci relationship and other arrangements having nothing to do with Fibonacci sequences. No credibility can be assigned to any claim that a particular number discloses the involvement of Fibonacci sequences.

**Table 1.** The results from querying the on-line search tool available at Sloane (2004) for the number of integer sequences containing specified short sequences derived from the primary Fibonacci sequence. Maximum number of sequence matches provided in response to a given query is 100

Query sequence	Total matches	Fibonacci-related sequences
1,2,3,5	100	9 (9%)
1,2,3,5,8	100	37 (37%)
1,2,3,5,8,13	79	41 (52%)
1,2,3,5,8,13,21	40	26 (65%)
1,2,3,5,8,13,21,34	26	22 (85%)

(2) Can the groupings of biological objects in small sets exhibiting consecutive numbers such as 2, 3, 5 and 8 or 3, 4, 7, and 11 be exclusively attributed to the operation of a Fibonacci sequence? In other words, is the appearance of biological objects in 2s, 3s and 5s sufficient to reveal the involvement of the primary Fibonacci sequence? An earlier section devoted to a primer on number sequences demonstrated that no small set should be assumed to represent only one number sequence, and this warning most certainly applies to small sets taken from Fibonacci sequences.

Sloane (2004) provides a query tool that allows the screening of a database of *c.* 100 000 sequences in order to identify all sequences containing a specified small number set. Table 1 shows that a miniscule proportion of the number sequences including the short sequence of 1, 2, 3 and 5 are related to Fibonacci sequences. Even the addition of 8 and 13 to this short sequence makes only 52% of the identified sequences related to Fibonacci sequences. Therefore, identifying a small set of consecutive numbers as belonging to a Fibonacci sequence is a necessary but not sufficient criterion for establishing the operation of the Fibonacci sequence in the biological pattern under investigation.

(3) Does the primary fractional Fibonacci sequence (2/1, 3/2, 5/3, 8/5, etc.) have unique mathematical properties that arise from its limit of  $\phi$ ? Perhaps special consideration should be granted to the numbers in the primary Fibonacci sequence, as opposed to the numbers in other Fibonacci sequences. I have already indicated above that the fractional sequences composed of primary Fibonacci numbers result in golden ratios of  $\phi$  and  $\phi^{-1}$  as their limits, and therefore it might seem reasonable to propose that the primary fractional sequences might have unique features attributable to their limits.

However, one must also be disabused of this appealing notion, because a fractional Fibonacci sequence

constructed from any two initial numbers chosen at random will inevitably converge on either  $\phi$  or  $\phi^{-1}$ , as is noted by several authors, including Thompson (1942), Huntley (1970) and Livio (2002). For example, using 4 and 87 as the initial numbers, the resulting fractional Fibonacci sequences are:

$$\frac{87}{4}, \frac{91}{87}, \frac{178}{91}, \frac{269}{178}, \frac{447}{269}, \frac{716}{447}, \frac{1163}{716}, \frac{1879}{1163}, \dots$$

and the reciprocal

$$\frac{4}{87}, \frac{87}{91}, \frac{91}{178}, \frac{178}{269}, \frac{269}{447}, \frac{447}{716}, \frac{716}{1163}, \frac{1163}{1879}, \dots$$

The 8th term is equal to 1.6156... in the first fractional sequence, and to 0.6189... in the reciprocal sequence, which illustrates just how rapidly fractional Fibonacci sequences (with an initial term of  $x_a/x_b$ ) converge on  $\phi$  (in the case of  $x_a > x_b$ ) or  $\phi^{-1}$  (in the case of  $x_a < x_b$ ). Moreover, all fractional Fibonacci sequences approach the powers of  $\phi$  as their limits following the same formulae as shown for the primary fractional sequences (Appendix Table A2). It should be obvious that specific numbers, even those in the primary Fibonacci sequence, have no special mathematical relationship with  $\phi$  or  $\phi^{-1}$ , but rather these limits are the inevitable outcome of the fractional Fibonacci formula.

The mathematical relationships described above have profound implications for any attempt to relate a set of grouped objects exhibiting some numbers from a primary fractional Fibonacci sequence to the underlying mechanism generating the biological pattern. First of all, it underscores the concept from the primer section that the formula is critical for defining any class of number sequences, including Fibonacci sequences. More specifically, it establishes that the limit  $\phi$ , and the mathematical properties associated with it, are solely attributable to the operation of the fractional Fibonacci formula, as opposed to being associated with the trivial numbers comprising any given fractional sequence. Therefore, the operation of a Fibonacci sequence can only be visualized in a biological pattern exhibiting two characteristics: (1) the biological objects are arranged in various groupings exhibiting different Fibonacci numbers, and (2) developmental transitions to other groups of different numbers must follow a discernible Fibonacci formula. Only if the pattern expresses both characteristics can an investigator argue for the likely involvement of a Fibonacci sequence.

What the reader needs to retain from this rather belaboured discussion is that just because some biological objects are grouped in a specific number found in the primary Fibonacci sequence, it does not mean that these objects are being arranged in accordance with the Fibonacci sequence. For example, let us say

that an organism is usually observed to produce a structure composed of five units. If this organism or related organism can also develop the same structure with either three or eight units, then we have much stronger evidence that the structure depends on the operation of a Fibonacci-based mechanism. However, if the occasional smaller and larger structures are composed of four and six units, respectively, then this structure is constructed without the apparent involvement of the Fibonacci sequence. We are now prepared to evaluate the question of whether phyllotactic patterning in plants can be ascribed to the operation of Fibonacci sequences.

## FIBONACCI NUMBERS AND PHYLLOTACTIC PATTERNS

In the phyllotaxis literature, it is often asserted the phyllotactic patterns result from the operation of the geometrical imperative of optimal packing or its equivalent. This assertion can be deconstructed into three sequential propositions:

1. Are the primordia of leaf homologues arranged according to the numbers composing the Fibonacci sequence?
2. Do the arrangements exhibiting Fibonacci numbers reveal the underlying operation of the Fibonacci formula?
3. Do the arrangements following the Fibonacci formula generate optimal packing?

In this section, the first two questions will be used to evaluate the organization of leaf primordia in the two principal types of phyllotactic arrangements observed in seed plants. The third question is deferred until the following section.

### PHYLLOTACTIC WHORLS

One common phyllotactic pattern is the whorl, where a group of leaf homologues, such as foliage leaves or floral organs, arise at the same node of a shoot axis. Many aquatic angiosperms, such as *Myriophyllum spicatum* L., *Anacharis canadensis* (Michx.) Planch. and *Ceratophyllum demersum* L., as well as some terrestrial plants are observed to develop foliage leaves in whorls of 3, 4 and 5. Most angiosperm flowers produce petals and other floral organs in whorls of 2, 3 and 5, or their multiples. Just to cite a few examples, almost all species in the Ranunculaceae and Rosaceae have 5 petals, whereas many species in the Liliaceae are characterized by 3 or 6 petals. Do these numbers disclose the role of the Fibonacci sequence in specifying the number of leaf homologues in each whorl, as is argued in the botanical literature (e.g. Church, 1920; Endress, 1987)? It should be clear from the previous

section that the critical evidence for evaluating this claim lies in the transitions to other whorls with different numbers of leaf homologues.

The evidence available from those plants with whorled foliage leaves is incontrovertible. Vegetative shoots are indeterminate structures with many nodes of foliage leaves so that it is relatively easy to identify and characterize whorled plants with different leaf numbers at their nodes. For example, McCully & Dale (1961) studied the heteroblastic changes in leaf number in successive whorls in the angiosperm *Hippuris* sp. L., which exhibits whorls ranging from 2 to 16 leaves. Their observations demonstrated that the number of leaves in successive whorls change by small increments of one or two leaves, with the leaf number being strongly correlated with the diameter of the shoot apex at the time of whorl initiation (Fig. 3). The

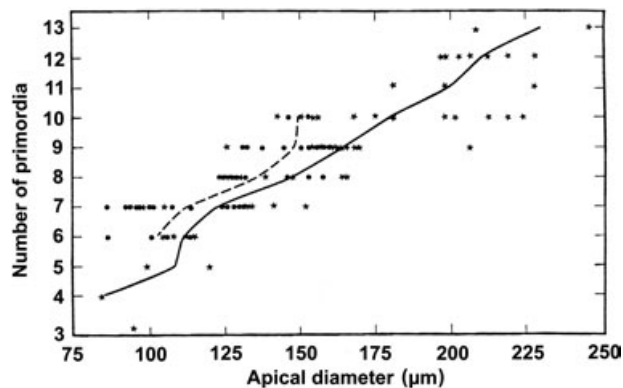


**Figure 3.** Relationship between the number of leaf primordia in the youngest whorl and the diameter of the apical dome. The solid circles and dotted line represent the observations on aerial shoots; the stars and solid line represent the observations on submerged shoots. The lines connect the mean diameters correlated with each leaf number. Redrawn with permission from McCully & Dale (1961).

whorled shoots of several species of the sphenopsid *Equisetum* L. exhibit similar changes in leaf number that are also related to apex diameter (Bierhorst, 1959). These studies establish that leaf numbers in vegetative whorls do not undergo heteroblastic changes in accordance with a discernible Fibonacci formula. Therefore, the Fibonacci sequence plays no apparent role in the generation of whorled phyllotaxis on vegetative shoots.

By contrast, flowers are determinate structures that are frequently composed of single whorls of each type of floral organ; therefore, it is generally impossible to observe developmental transitions in floral organ whorls such as those observed in foliage leaf whorls on vegetative shoots. However, there are two reasons for concluding that the Fibonacci sequence is also uninvolved in the specification of whorled phyllotaxis in flowers. One, ever since Goethe (1790), plant morphologists have recognized that all determinate lateral organs, such as foliage leaves and floral organs, are homologous structures. It is noteworthy that this morphological concept has received molecular confirmation insofar as triple mutations in the ABC class genes cause the floral organs to revert to leaf-like phenotypes (Coen & Meyerowitz, 1991). Thus, one might reasonably hypothesize that phyllotactic arrangements of whorled floral organs are mediated by non-Fibonacci mechanisms related to those operating in leaf whorls. Two, several *Arabidopsis* mutants exhibit altered numbers of floral organs as compared with wild-type plants. Wild-type *Arabidopsis* flowers develop concentric whorls of 4 sepals, 4 petals, 6 stamens and 2 carpels, whereas these mutant flowers develop more or fewer organs in several whorls (Table 2). For example, *wus* flowers tend to have 3 or 4 sepals, 3 or 4 petals, and 0–3 stamens (Laux *et al.*, 1996). By contrast, *pan* flowers often develop 5 and sometimes 6 organs in the three outer whorls (Running & Meyerowitz, 1996). One cannot assign the

**Table 2.** The number of sepals, petals and stamens in wild-type and mutant flowers of *Arabidopsis thaliana*

Mutant name or TAIR number	Floral organ number			Reference
	Sepals	Petals	Stamens	
wild-type	4	4	6	
CS2310	3–4	3	3–4	TAIR (2004)
<i>petal loss (ptl)</i>	4	0–3	6	Griffith <i>et al.</i> (1999)
<i>wuschel (wus)</i>	3–4	3–4	0–3	Laux <i>et al.</i> (1996)
<i>perianthia (pan)</i>	5	5	5	Running & Meyerowitz (1996)
CS2292	4–5	4–5	?	TAIR (2004)
CS2289	?	5–6	6–7	TAIR (2004)
<i>clavata1 (clv1)</i>	4–6	4–6	6–10	Leyser & Furner (1992), Clark <i>et al.</i> (1993)
<i>clavata3 (clv3)</i>	5–6	5–6	9–11	Clark <i>et al.</i> (1995)

observed differences between organ numbers in wild-type vs. mutant flowers to the operation of any obvious Fibonacci formula. Moreover, the changes in floral organ number are directly correlated with floral meristem size in certain mutants (*wus*: Laux *et al.*, 1996; *clv1*: Clark, Running & Meyerowitz, 1993; *clv3*: Clark, Running & Meyerowitz, 1995) but not in others (*pan*: Running & Meyerowitz, 1996; *ptl*: Griffith, da Silva Conceição & Smyth, 1999), so that a related mechanism may be partially responsible for specifying whorl number in both foliage leaves and floral organs.

The unrestrained tendency to visualize the Fibonacci sequence in botanical patterns has led to some rather ill-conceived interpretations about how various flowers produce their petals in whorls of primary Fibonacci numbers ranging from 1 to 89, as are commonly cited in the mathematics literature (e.g. Huntley, 1970; Koshy, 2001) and in popular publications (e.g. Garland, 1987; Britton, 2003; Knott, 2004). These exuberant claims do not pass close scrutiny for several reasons, not the least of which is that the structures cited are often not petals at all. For example, Britton (2003) illustrates the calla lily as an example of a flower with a single petal; it turns out that this structure is an enlarged bract known as the spathe that grows around the condensed inflorescence composed of many small flowers. Various members of the Asteraceae are almost universally cited as having petal numbers equal to the primary Fibonacci numbers of 8, 13, 21, 34, 55 and 89. Of course, these so-called petals are more properly referred to as ray florets, which do not arise in true whorls but rather in compressed spirals called pseudowhorls. Nor do the ray florets of the Asteraceae appear to meet any rigorous standard for exhibiting the operation of the Fibonacci formula. As an initial survey, I counted the number of ray florets on 100 inflorescences of several Asteraceae species readily available in Spring Silver, MD (Fig. 4). In a clone of *Rudbeckia fulgida* Ait. 'Goldstrum' growing in my back garden, the mean number of ray florets per capitulum for 100 capitula was 12.82, which happens to fall quite close to the primary Fibonacci number of 13, as reported by Britton (2003). However, Figure 4 illustrates that the ray florets on individual capitula ranged from 10 to 15 in number. By contrast, 100 capitula of a large *Chrysanthemum morifolium* L. plant purchased from a local nursery exhibited a mean number of ray florets per capitulum of 25.68 and a range of 20–36 ray florets on different capitula. A population of *Cichorium intybus* L. growing along an exposed roadside displayed a mean of 16.52 ray florets per capitulum ranging from 13 to 20 florets on different capitula. It is clear from this small sample that different Asteraceae species exhibit a normal distribution of ray florets in their capitula, with the means apparently approaching a primary

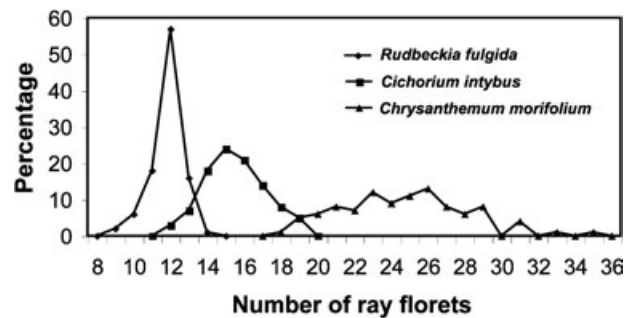


**Figure 4.** Distribution of the number of ray florets in 100 capitula of three Asteraceae species: *Rudbeckia fulgida* (mean of 12.82 florets per capitulum), *Cichorium intybus* (mean of 16.52 florets per capitulum) and *Chrysanthemum morifolium* (mean of 25.68 florets per capitulum).

Fibonacci number in certain species. However, there is no cogent evidence from Figure 4 that such occasional coincidences have any biological significance, and thus it appears that the Fibonacci sequence does not participate in the regulatory mechanism specifying ray floret number.

In conclusion, the evidence on whorled phyllotaxis presented here can be used to address the three propositions stated at the beginning of this section. Whorled phyllotaxes do satisfy the first proposition insofar as the whorls on both vegetative and reproductive shoots are often composed of a primary Fibonacci number of leaf homologues. However, the evidence does not satisfy the other two propositions. Developmental transitions of foliage leaf whorls and genetic manipulations of floral organ whorls do not follow discernible Fibonacci formulae. Therefore, the whorled arrangements of foliage leaves and of floral organs do not depend on a Fibonacci-based mechanism. Consequently, whorled phyllotaxis cannot result from the operation of a hypothetical geometrical imperative for optimal packing.

#### PHYLLOTACTIC SPIRALS

In many terrestrial seed plants, the foliage leaves on vegetative shoots are routinely observed to develop in opposing clockwise and anticlockwise spirals called parastichies. If the leaves are assigned a number in the order of their origin, then the intervals in the numbers between successive leaves in these spiral pairs are typically related to the primary Fibonacci sequence (for illustrations, see Williams, 1975). For example, a shoot apex producing leaf primordia in two opposing parastichies with primordium intervals of  $n + 2$  and  $n + 3$  is said to exhibit the (2,3) phyllotaxis. This arrangement is roughly equivalent to the 2/5 phyllotactic fraction of mature shoots, where the gen-

**Table 3.** Distribution of spiral phyllotaxes in angiosperms. Phyllotactic patterns were measured as contact parastichies in apical cross-sections. The divergence angles calculated for the contact parastichies assume an orthogonal arrangement of those parastichies. The data for reproductive shoots were compiled from the arrangements of floral organs in individual flowers and those of flowers in inflorescences. n.d., no data collected for these spirals. Adapted from Fujita (1938), as tabulated by Williams (1975)

Phyllotactic patterns	Divergence angles (°)	Vegetative shoots	Reproductive shoots
Primary Fibonacci spirals			
(1,1)	180	n.d.	n.d.
(1,2)	120	45	–
(2,3)	144	335	35
(3,5)	135	53	43
(5,8)	138.46	4	25
(8,13)	137.14	1	12
(13,21)	137.65	–	11
(21,34)	137.45	–	2
(34,55)	137.53	–	–
Accessory Fibonacci spirals		1	29
Bijugate spirals		–	8
Total shoots		439	166
Species represented		411	121

erative spiral is seen to complete two circuits around the stem for every five leaves.

Frequently, the parastichies used to characterize spiral phyllotaxis are the so-called contact parastichies or those derived from drawing spirals through adjacent primordia in direct contact. Fujita (1938) surveyed the distribution of spiral phyllotaxis in the vegetative and reproductive axes of seed plants. In angiosperms, c. 80% of all spiral phyllotaxes are reportedly characterized by contact parastichies in the (2,3) pattern (Table 3). Most other spiral phyllotaxes on vegetative shoots exhibit either the (1,2) or the (3,5) arrangement of contact parastichies, although the common distichous (1,1) phyllotaxis was apparently excluded from this survey. Thus, Fibonacci spirals represent the predominant pattern among all possible spirals in this survey as well as in other surveys (Church, 1920; Jean, 1994). One cautionary note is that contact parastichies are dependent on primordial shape, and thus they may not provide an accurate measure of relative primordial position. Richards (1948, 1951) quite rightly emphasized that the position of successive primordia is completely specified in the transverse plane by the divergence angle and the plastochron ratio, i.e. the relative radial distances of two successive primordia. In Richard's analysis, primary attention is granted to those pairs now known as conspicuous parastichy pairs (Adler, 1974; Jean, 1994) whose intersection most closely approaches a 90° angle. It turns out that these conspicuous parastichy pairs also exhibit adjacent Fibonacci numbers, and moreover they will usually, but not always, coincide

with the more obvious contact parastichy pairs (for discussion, see Williams, 1975; Jean, 1994). Irrespective of the approach used to identify the parastichy pairs, it is inescapable that the spiral phyllotaxes of vegetative shoots are overwhelmingly characterized by low Fibonacci numbers.

Reproductive shoots display spiral patterns on two different morphological levels, namely floral organs in individual flowers and flowers in inflorescences (Fujita, 1938; Endress, 1987). In comparison with vegetative shoots, reproductive shoots show a much greater distribution of spiral phyllotaxes, ranging from (2,3) to (34,55) patterns, with the mode being (3,5) (Table 3). Such flowers as water lilies and magnolias with high numbers of floral organs tend to develop their organs in spiral patterns exhibiting primary Fibonacci numbers; for example, the flowers of *Magnolia obovata* Thunb. exhibit (13,21) patterns of stamens and of carpels (Fujita, 1938). Because floral organs are presumably homologous to foliage leaves, these observations suggest that spiral phyllotaxis of both organ types may depend on related patterning mechanisms. However, the floral organs of certain flowers including *Michelia fuscata* (Andr.) Blume (Tucker, 1961) exhibit spiral patterns that do not follow the primary Fibonacci sequence (Table 3). A plausible explanation of these divergent patterns lies in the much higher rate of floral organ initiation, which may also account for the occasional appearance of chaotic arrangements (Endress, 1987).

Lastly, the flowers on the inflorescences of most angiosperms, such as *Capsella bursa-pastoris* (L.)

Medic. and *Antirrhinum majus* L., are usually positioned in spiral patterns exhibiting low Fibonacci numbers (Table 3; Fujita, 1938). It is quite likely that the mechanism specifying the position of individual flowers may also be related to those operating in foliage leaf and floral organ phyllotaxis. It turns out that flowers tend to arise in the axils of leaf-like bracts, which are also considered as being leaf homologues. Because these bracts are usually arranged in spiral patterns, the result is that the entire inflorescence tends to display spiral phyllotaxis. It is worth pointing out that the phyllotaxis literature tends to grant disproportionate attention to the few extraordinary cases of reproductive structures displaying high Fibonacci numbers such as the ovulate cones of various conifers, the multiple fruit of the pineapple *Ananas comosus* (L.) Merr., and the disc flowers on the capitula of the Asteraceae. For example, pineapple fruits are typically characterized by either (8,13) or (13,21) parastichies. It is obvious that the spiral organization of conifer cones and pineapple fruits reflects the positioning of the evident bracts subtending the individual units in these reproductive structures. The extreme (34,55) phyllotaxis reported in Table 3 is exhibited by disc florets on the capitulum of the sunflower *Helianthus annuus* L. (Fujita, 1938). The capitula of the Asteraceae are traditionally interpreted as being condensed shoot systems, and it is therefore expected that their organization is dependent on the same developmental mechanisms operating in vegetative shoots (Burt, 1978). Indeed, many Asteraceae species, including *Helianthus annuus* and other members of the tribe Heliantheae, have retained a subtending bract called the palea or receptacular scale at the base of each floret (P. K. Endress, pers. comm.), which is presumably involved in the positioning of the florets on the capitulum. (The palea may be reduced to form receptacular bristles or is completely missing in other Asteraceae species, but it is unlikely that these species would have evolved novel mechanisms for positioning their florets.) In conclusion, it seems quite reasonable to make the broad generalization that the spiral phyllotaxes of vegetative shoots, flowers and inflorescences are all generated by related mechanisms acting to specify the positions of leaf homologues.

Even though spiral phyllotaxes are routinely characterized by Fibonacci numbers, one must also show that developmental transitions to other spirals follow a Fibonacci formula in order to confirm the operation of Fibonacci-based mechanisms in spiral phyllotaxis. The vegetative shoots of most plants exhibit a stable, characteristic spiral phyllotaxis following the initiation of the first few foliage leaves; however, certain plants do undergo phyllotactic transitions following the Fibonacci formula throughout vegetative growth. Just to cite one example, the vegetative shoot of

*Linum usitatissimum* L. undergoes a heteroblastic increase in the numbers of its Fibonacci spirals (Williams, 1975). The 4-day-old seedling exhibits a decussate pattern that is originally established in the embryo (Fig. 5). Subsequent leaf primordia are arranged in a (3,5) phyllotaxis in the apices of 8- and 15-day-old plants. Then the shoot apex starts producing new primordia at a much higher rate, resulting in a (5,8) phyllotaxis in 22-day-old apices. In the apices of the 50-day-old plants with over 200 leaves, the contact parastichies are still arranged in the (5,8) pattern, but the conspicuous parastichies are seen to approach the (8,13) pattern (Fig. 5). Various species in the Magnoliaceae exhibit stepwise transitions following the Fibonacci formula in the spiral phyllotaxes of stamens vs. carpels (Fujita, 1938). For instance, the stamens of *Magnolia grandiflora* L. arise in an (8,13) phyllotaxis, but its carpels change to a (13,21) pattern. By contrast, the reproductive organs of *Liriodendron tulipifera* L. undergo the opposite transition in parastichy numbers. Comparable Fibonacci-based transitions are also seen in inflorescences, such as sunflower capitula, where the transitions depend on capitulum size and flower position. Although the disc flowers are typically observed to arise in a (34,55) pattern in the outer regions of normal-sized sunflower capitula, small capitula exhibit either (13,21) or (21,34) patterns, and larger capitula exhibit higher Fibonacci spirals in step-wise increases to a maximum of the (144,233) pattern (Jean, 1984). It is also observed that the disc flowers on a normal capitulum proceed from a (34,55) phyllotaxis at the periphery, to a (21,34) pattern in the intermediate region, and then to lower Fibonacci spiral phyllotaxes near the centre (Thompson, 1942; Richards, 1948; Williams, 1975). In oilseed sunflower hybrids, large capitula displaying the peripheral (89,144) phyllotaxis are also seen to undergo step-wise Fibonacci decreases toward their centres (Palmer, 1998). In marked contrast to whorled phyllotaxis, the evidence presented here means that even this skeptical author cannot cogently argue against the characterization of spiral phyllotaxis of both vegetative and reproductive shoots in terms of the formula for the primary Fibonacci numbers.

#### GEOMETRICAL IMPERATIVE OF OPTIMAL PACKING

However, there remains the question of whether or not such spiral arrangements are attributable to the leaf primordia being positioned in optimal packing. Several mathematical models have employed close packing, contact pressure or their equivalents as the causal mechanism for generating spiral patterns exhibiting Fibonacci numbers (e.g. van Iterson, 1907; Erickson, 1973; Adler, 1974; Ridley, 1982a). In general, these

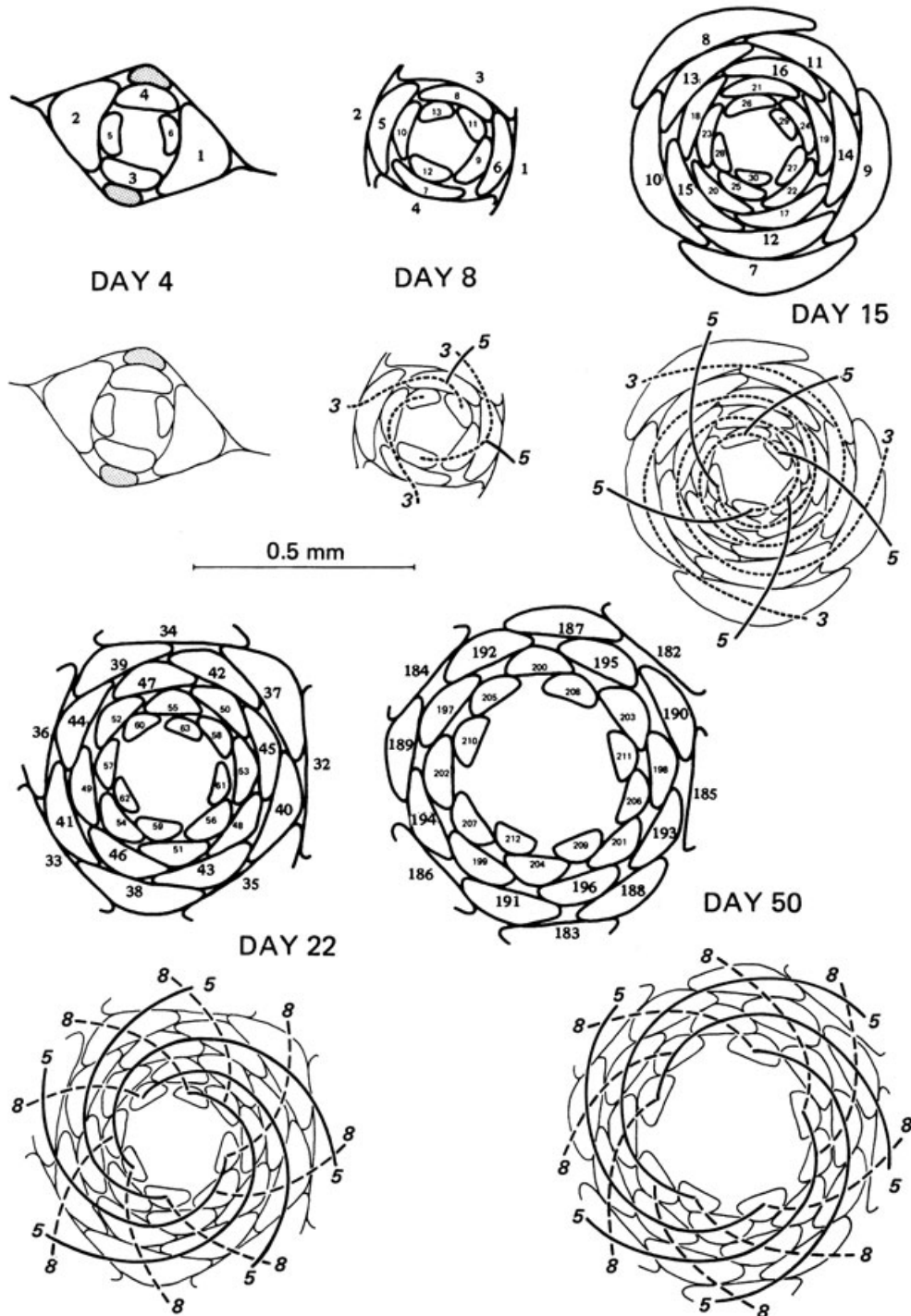


**Figure 5.** Transverse sections of shoot apices of *Linum usitatissimum* at different developmental stages. For each stage, the top drawing indicates the number of each leaf primordium on the apex, starting with the first epicotylar primordium as number 1, and the bottom drawing shows the corresponding contact parastichies superimposed on the apex. Day 4 apex exhibits a decussate pattern that is originally established in the embryo; the stippled structures represent lateral buds that have developed in the axils of the cotyledons. Subsequent leaf primordia on the day 8 and 15 apices are initiated in a (3,5) phyllotaxis, but younger leaf primordia arise in a (5,8) phyllotaxis on the day 22 apex. On the day 50 apex, the contact parastichies are still arranged in a (5,8) pattern, but the conspicuous parastichies approach an (8,13) pattern. Redrawn with permission from Williams (1975).

models are designed to evaluate the relationship between the angular divergence of successive units of uniform size and the packing efficiency of the overall structure. This research has convincingly shown that a generative spiral with a divergence angle equal to the so-called ideal or Fibonacci angle of  $137.5^\circ$  results in optimal packing. Moreover, some efforts have successfully generated realistic models of sunflower capitula that can even show decreased Fibonacci numbers toward the centre (e.g. Vogel, 1979; Rivier *et al.*, 1984). This work has sparked renewed interest in applying crystallographic approaches to phyllotaxis (Rivier *et al.*, 1984; Jean, 1994; Mackay, 1998; Selvan, 1998). Lastly, a modified version of an optimal packing argument is sometimes used as a *deus ex machina* to explain what appears inexplicable by even those workers whose research does not emphasize Fibonacci numbers. For example, Green (1999: 1064–1065) invoked relative packing as a rather contrived rationale to account for the switch between spiral and whorled patterns. Thus, it seems entirely appropriate here to attempt a critical analysis of the putative role of optimal packing in spiral phyllotaxis.

#### A SIMPLE MODEL

Underlying most proposed packing mechanisms is the implicit assumption that golden geometry expressed in the form of the Fibonacci angle of  $137.5^\circ$  is operating in phyllotactic patterning. Both theoretical considerations and direct observations invalidate that assumption. For instance, as a simple graphical exercise, let us examine the relative packing in a subdivided golden rectangle vs. other subdivided rectangles with the aspect ratios corresponding to the common contact parastichies observed in spiral phyllotaxis ( $1/1$ ,  $1/2$ ,  $2/3$ ,  $3/5$ ,  $5/8$  and  $8/13$ ) and the resulting divergence angles ( $180^\circ$ ,  $120^\circ$ ,  $144^\circ$ ,  $135^\circ$ ,  $138.46^\circ$  and  $137.14^\circ$ ) (Table 3). It is assumed in the initial presentation of this exercise that the contact parastichies can be used to estimate the divergence angles of actual leaf primordia arising on the shoot apex. The limitations of this assumption are addressed in the following section.

As described earlier, a unique property of a golden rectangle (with the aspect ratio of  $1/\phi$ ) is that can be subdivided into a square and a smaller golden rectangle *ad infinitum*, with each successive rectangle exhibiting the same proportions as the previous rectangle. It turns out that if circles are inscribed in the squares, then a subdivided golden rectangle, as illustrated in Figure 6, appears quite reminiscent of two-dimensional projections of genuine shoot apices. First of all, the ability of the golden rectangle to undergo repeated subdivisions is highly suggestive of the indeterminate growth of most vegetative and

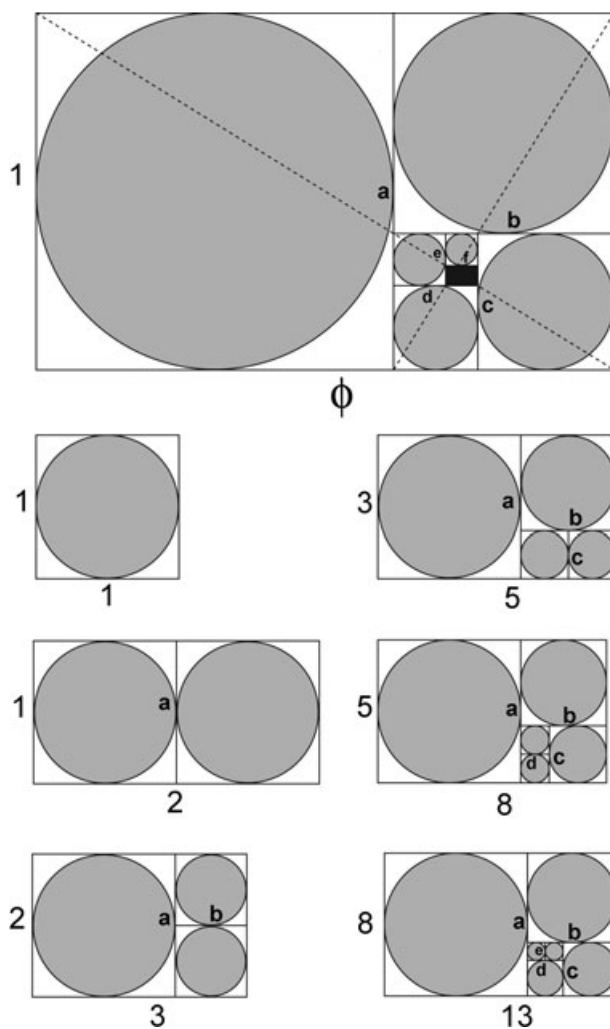


**Figure 6.** Modelling results from one process of subdividing the golden rectangle and other rectangles with aspect ratios corresponding to the most common contact parastichies. The subdivision process illustrated in this figure involved first cutting off the largest possible square in the original rectangle and then repeating the process in the remaining portion of the rectangle until the entire rectangle is occupied by the squares. The subdividing lines are marked by lower-case letters in the order of their insertion. Circles representing leaf primordia (grey shading) are inscribed in the squares. The space between the squares and the circles is defined as inscribed free space (unshaded areas). After six subdivisions, the golden rectangle contains an unsubdivided centre (black shading) in the shape of a golden rectangle that can further be subdivided *ad infinitum*. The dashed lines in the golden rectangle converge on the 'Eye of God'. The other rectangles can undergo only a finite number of these subdivisions until they are entirely occupied by the squares.

reproductive shoots. The resulting primordia drawn as circles (or other realistic shapes) are seen to maintain this shape as one proceeds from the 'older', i.e. larger and first-drawn, primordia near the edges of the golden rectangle to the 'younger', i.e. smaller and later-drawn, primordia closer to its centre. Even the expression 'Eye of God' seems a rather appropriate name for the apical dome, at least to this botanist! Of course, there are several noteworthy differences: (1) a subdivided golden rectangle exhibits a divergence angle of  $90^\circ$ , as opposed to the larger angles observed in the generative spirals of most plants, and (2) the central region of a subdividing golden rectangle is not restored to its original size following each subdivision, as is the apical dome of a real shoot apex. Nevertheless, a subdivided golden rectangle is realistic enough to allow us to evaluate the packing efficiencies of two-dimensional projections of actual apices expressing different contact parastichies.

A subdivided golden rectangle has several other advantages as a model for phyllotactic patterning. This model provides an explicit definition of optimal packing that is pertinent to actual phyllotaxis. In particular, optimal packing can now be defined as having two independent properties: (1) self-regeneration, i.e. each subdivision of the golden rectangle results in the formation of a new square and/or its inscribed form plus a smaller golden rectangle capable of another such subdivision; and (2) tight packing, which is expressed as no residual free space following each subdivision into the largest possible square and the smaller golden rectangle. Furthermore, the model of subdivided rectangles offers the opportunity to determine whether the optimal packing characteristic of a subdivided golden rectangle is also exhibited by other subdivided rectangles constructed from the contact parastichies representing the most common phyllotaxes. In other words, this model allows us to test whether spirals exhibiting the fractional Fibonacci sequence have the same geometrical properties as do the spirals arising from  $\phi$ , the limit of that sequence.

The largest possible square drawn in the golden rectangle depicted in Figure 6 will completely fill the rectangle except for the remaining smaller golden rectangle. In Figure 6, this subdivision is repeated six times, which leaves an unsubdivided central region that retains the same proportions as the original golden rectangle. Because each subdivision regenerates a smaller rectangle with the same aspect ratio as the original rectangle, this subdivision can be repeated *ad infinitum*, with no residual free space being left over within the original boundaries of the golden rectangle. Thus, the golden rectangle meets the criterion for tight packing given above. If a more realistic form is inscribed in the squares to represent leaf primordia, then a second type of free space is located

between the boundaries of each inscribed form and its surrounding square. This free space is called inscribed free space in order to differentiate it from any potential residual free space associated with the initial drawing of the largest squares. For the sake of simplicity, this paper uses inscribed circles to represent leaf primordia. In a subdivided golden rectangle, the inscribed free space outside the circles but within the squares is equal to the ratio of the areas of a circle and of a square, which equals  $\pi/4$  or 21.46% of the total area of the golden rectangle.

Figure 6 also illustrates the results from drawing the largest possible squares in other rectangles whose aspect ratios ( $1 \times 1$ ,  $1 \times 2$ ,  $2 \times 3$ ,  $3 \times 5$ ,  $5 \times 8$ ,  $8 \times 13$ ) represent the most common spiral phyllotaxes. Using the  $2 \times 3$  rectangle as an example, the first subdivision is seen to cut off the largest possible square of  $2 \times 2$  dimensions and leave a  $1 \times 2$  rectangle. This smaller rectangle is, in turn, subdivided into two largest possible squares of  $1 \times 1$  dimensions, with the result that no residual free space is left within the original rectangle. Inscribe circles within the squares of this subdivided rectangle results in 21.46% inscribed free space. As this rectangle, just like a subdivided golden rectangle in Figure 6, has no residual free space, it exhibits tight packing. However, unlike the golden rectangle, this rectangle does not exhibit the property of self-regeneration because a finite number of largest possible squares consumes the entire rectangle. Although the subdivided rectangles with other initial dimensions in Figure 6 undergo a variable number of such subdivisions ranging from zero in the  $1 \times 1$  square to five in the  $8 \times 13$  rectangle, the subdivisions of each rectangle consume the entire rectangle with no residual free space and 21.46% inscribed free space. It can therefore be concluded that using the largest possible square to subdivide any rectangle constructed from the fractional primary Fibonacci sequence results in tight packing without any capacity for self-regeneration. The latter limitation means that these particular rectangles are unrealistic models of actual apices, and thus they will not be considered further.

By contrast, the order of the steps in the subdivision process can be reversed so that first a smaller rectangle of the same proportions as the original rectangle is cut off at a  $90^\circ$  divergence angle and then the largest possible square with its inscribed circle is drawn in the remaining area. This reversed order has no effect on the appearance of a subdivided golden rectangle so that it continues to exhibit both tight packing and self-regeneration (Fig. 7). However, this reverse does alter the appearances of the subdivided rectangles, the dimensions of which are taken from the contact parastichies corresponding to the fractional primary Fibonacci sequence, as is also illustrated in Figure 7.

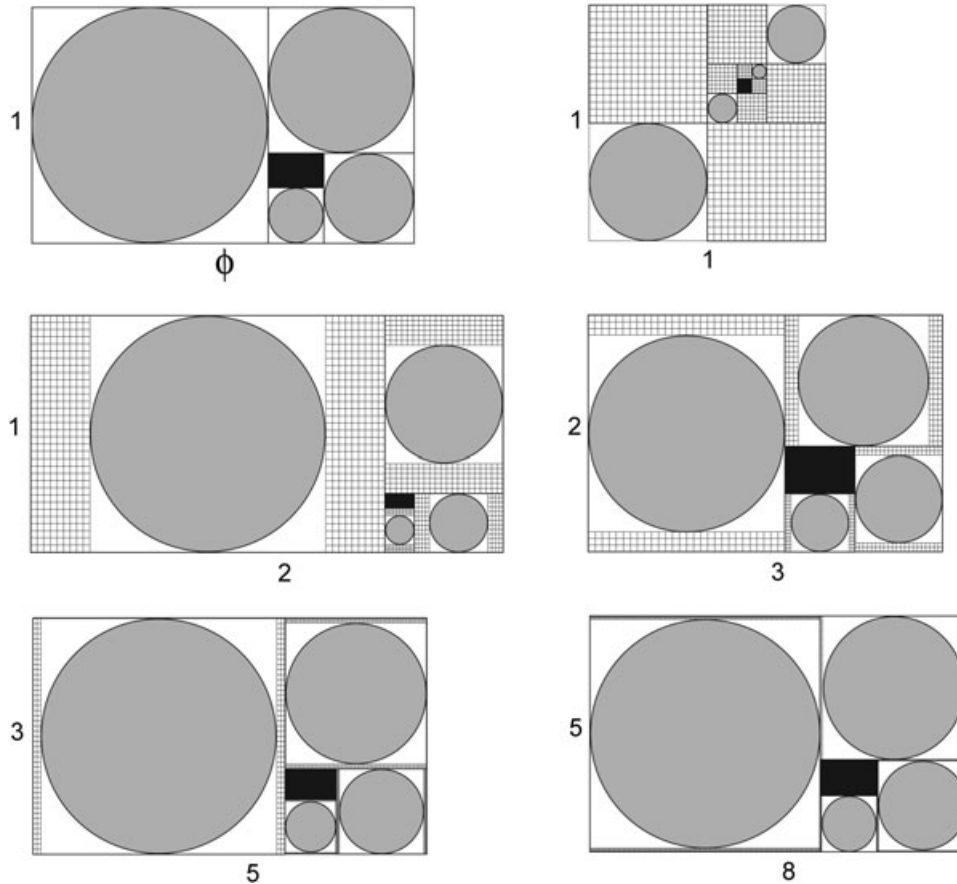


**Figure 7.** Modelling results from another process of subdividing the golden rectangle and other rectangles with aspect ratios corresponding to the most common contact parastichies. The subdivision process involved first cutting off the largest possible rectangle with the same aspect ratio of the original rectangle and at a divergence angle of  $90^\circ$ , and then drawing the largest possible square in the remaining space. The procedure used to subdivide the  $1 \times 1$  square is described in the text. Only the first four subdivisions are shown for each rectangle. Circles representing leaf primordia (grey shading) are inscribed in the squares. The space between the squares and the circles is defined as inscribed free space (unshaded areas). In each subdivision, the space left over after drawing the largest possible square is defined as residual free space (grid shading). Because every subdivision regenerates a rectangle with the same aspect ratio as the original rectangle, the unsubdivided centre (black shading) remaining in all rectangles can be subdivided *ad infinitum*. The calculated values for free space in the subdivided rectangles are presented in Table 4.

**Table 4.** Calculated values for free space in the rectangles depicted in Figure 7 after being subdivided *ad infinitum*. The rectangle with an aspect ratio of  $34/55$  was not illustrated there. For definitions, see the legend to Figure 7

Rectangle (aspect ratio)	Residual free space (%)	Inscribed free space (%)	Total free space (%)
$1/\phi$ (golden)	0.00	21.46	21.46
1/1	66.67	7.15	73.82
1/2	33.33	14.31	47.64
2/3	16.67	17.88	34.55
3/5	6.25	20.12	26.37
5/8	2.50	20.92	23.42
34/55	0.05	21.45	21.50

Table 4 presents the calculations of residual and inscribed free space for these subdivided rectangles. In the  $2 \times 3$  rectangle, every subdivision results in a smaller rectangle whose sides maintain the  $2 \times 3$  proportions, and thus this rectangle is capable of self-regeneration *ad infinitum* in a manner identical to this process in the golden rectangle. However, the largest possible square does not fill in the other part of each subdivision, with the consequence that 16.67% residual free space is left within the boundaries of the original rectangle. Thus, this rectangle does not exhibit tight packing. Owing to the absence of tight packing, the inscribed free space of 17.88% is less than the maximum of 21.46% achievable in any rectangle displaying tight packing.

This same process can also be used to subdivide the other rectangles in Figure 7 so that each one exhibits self-regeneration *ad infinitum*. In the first step of each subdivision, all the rectangles can be subdivided to generate one and only one rectangle of the same proportions, but an infinite number of possible squares regenerating the  $1 \times 1$  square can be drawn within its original boundaries. For illustrative purposes, the regenerating squares within the  $1 \times 1$  square are drawn with their dimensions being one-half the dimensions of the available space at each subdivision. Then the residual free space ranges from 66.67% in the  $1 \times 1$  square as drawn to 2.50% in the  $5 \times 8$  rectangle (Table 4). Conversely, the inscribed free space is lowest in the  $1 \times 1$  square at 7.15% and highest in the  $5 \times 8$  rectangle at 20.92%. Because the subdivisions of these rectangles illustrated in Figure 7 must inevitably produce residual free space, they are not characterized by tight packing. Other rectangles constructed from higher terms in the fractional sequence can approach, but do not achieve, perfect tight packing; for example, in the  $34 \times 55$  rectangle (model not shown), the residual free space is equal to 0.05% of the total rectangle. In essence, in the case of all rectangles with aspect ratios representing contact parastichies, a subdivision process regenerating the original aspect ratio will necessarily preclude tight packing. It turns out that this statement is also true for all other rectangles except the golden rectangle (data not shown). Thus, optimal packing, which is defined here as the simultaneous expression of self-regeneration and tight packing, can only be achieved by those arrangements manifesting some type of golden geometry. If the leaf primordia in spiral phyllotaxes are not positioned with a divergence angle of  $137.5^\circ$ , then it follows from this graphical exercise that their arrangement is not attributable to the hypothetical operation of a global geometrical imperative of optimal packing.

#### OTHER CONSIDERATIONS

Of course, the above analysis assumes that contact parastichies are orthogonal to each other such that the divergence angles can be calculated as shown in Table 3. This is true in only exceptional cases where the leaf primordia are initiated in superimposed orthostichies. However, the converse assumption that the primordia initiated in Fibonacci spirals are arranged in divergence angles equal to the golden angle of  $137.5^\circ$  is also false. Most apices with (1,1) or (1,2) phyllotaxis display divergence angles that are much closer to the expected values of  $180^\circ$  and  $120^\circ$ , respectively (e.g. Williams, 1975: 30). Surprisingly, the literature contains few reliable measurements of divergence angles in shoot apices with higher Fibonacci numbers (for critical evaluation, see Jean,

1994: 111–113, 317–320). Maksymowych & Erickson (1977) performed a meticulous study on the (2,3) phyllotaxis of vegetative apices of *Xanthium pensylvanicum* Wallr. They reported that the mean divergence angles of leaf primordia on 8 apices was  $139.1^\circ$ , with a range of  $135.5$ – $143.4^\circ$ . The divergence angles within individual apices exhibited much greater ranges: for example, the apex cited above with a low mean angle of  $135.5^\circ$  had individual angles ranging from  $124^\circ$  to  $140^\circ$ . Clearly, these divergence angles did not correspond to the expected angle of  $144^\circ$ . However, the primordia were also not positioned according to the Fibonacci angle of  $137.5^\circ$  so that they were not exhibiting optimal packing.

This interpretation that optimal packing can only be achieved by golden geometry is strongly supported by Ridley's (1982b) effort to model sunflower capitula with different divergence angles (Fig. 8). The capitulum model constructed with the Fibonacci angle as its divergence angle resulted in a packed arrangement resembling prior efforts using the same constraint (Vogel, 1979). However, the capitula constructed with divergence angles equal to either  $137.45^\circ$  or  $137.92^\circ$  exhibited well-ordered, but rather loosely packed models, thereby showing that even slight variation from the Fibonacci angle disrupted optimal packing (for another example, see Prusinkiewicz & Lindenmayer, 1990: 101). It is difficult, if not impossible, to imagine any biological system being capable of organizing itself with such discriminating accuracy as a direct response to a hypothetical geometrical imperative for optimal packing. It seems more likely that the spiral phyllotaxes observed in the sunflower capitulum and other examples with higher Fibonacci numbers are the outcome of some biological process, the consequence of which is that such structures tend to approach optimal packing.

Lastly, several workers have hypothesized that plants position their leaves in response to the selection pressure to maximize photosynthesis. Spiral phyllotaxes with Fibonacci numbers are thus proposed to represent the optimal arrangement for minimizing how much younger leaves might shade older leaves on the same axis (e.g. Wright, 1873; Leigh, 1972; King, Beck & Lüttge, 2004). These arguments are weakened by the unrealistic assumptions that the sun is always located at its zenith (or the plants are growing perpendicular to a fixed light direction) and that leaves are not capable of adjusting their relative positions following their initiation, as was noted by Thompson (1942). Even more decisive are the computer simulations of the capacity of model plants with different phyllotactic fractions (and hence different divergence angles) to absorb light (Niklas, 1988, 1998). His simulations examined almost all realistic factors affecting light reception, including morphological features, lat-

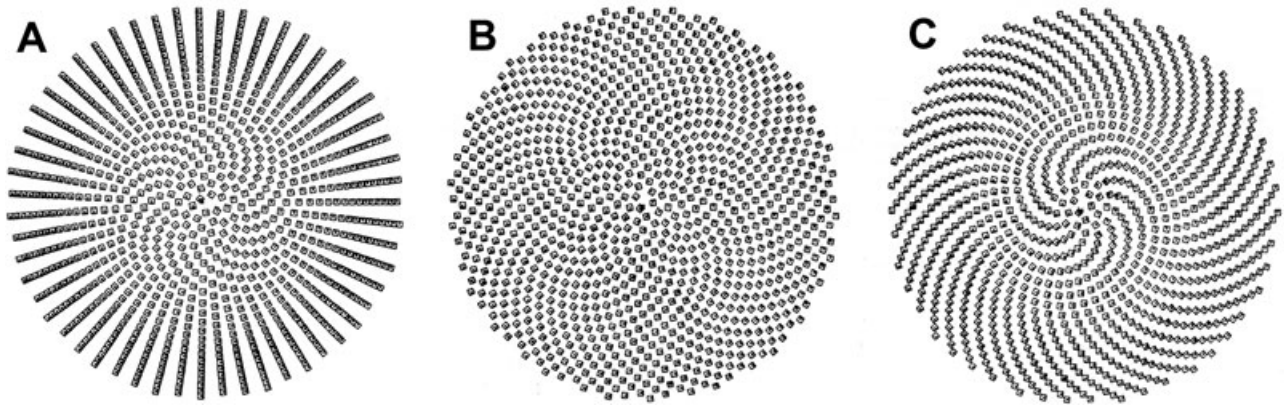


**Figure 8.** Packing efficiencies of model sunflower capitula constructed with different divergence angles. The models in panels A, B and C employed divergence angles equal to  $137.45^\circ$ , the golden angle of  $137.51^\circ$  and  $137.92^\circ$ , respectively. All three capitula display well-ordered arrangements of individual units, but only the capitulum constructed with the golden angle exhibits tight packing of those units. Redrawn with permission from Ridley (1982b).

itude, season and time of day, and they showed that most model plants except for rosette morphs with narrow leaves could potentially compensate for any negative effects of leaf overlap due to phyllotactic pattern by altering leaf shape, leaf orientation and/or internode length. Finally, these arguments about minimal overlap suffer from the logical error of confusing the proximate cause (i.e. developmental mechanism generating phyllotactic patterns) from the ultimate cause (i.e. selection pressures acting on those patterns). Among others, Goodwin (1994) has emphasized that natural selection by itself does not generate biological form but rather acts to stabilize the most adapted forms.

In conclusion, the considerations presented in these two sections on optimal packing demonstrate that the common spiral phyllotaxes expressing low Fibonacci numbers do not exhibit optimal packing, which implies that a geometrical imperative related to optimal packing cannot be operating to specify primordial position in such phyllotaxes. The infrequent spiral phyllotaxes expressing higher Fibonacci numbers are seen to approach a state of optimal packing. However, because it is likely that the same biological processes are specifying primordial position in all phyllotactic spirals, the tighter packing observed in higher Fibonacci spirals must be a secondary consequence of those processes.

#### IS PHYLLOTACTIC PATTERN GENERATED AS THE CONSEQUENCE OF UNDERLYING BIOLOGICAL PROCESSES?

Of course, a satisfying answer to this question requires the complete characterization of the biologi-

cal processes specifying phyllotactic pattern. This subject is the focus of considerable theoretical and experimental research, which extends beyond the topic of this paper (for reviews, see Jean, 1994; Lyndon, 1998). What I shall briefly discuss here is a promising approach based on recent research in physics, modelling, physiology and molecular genetics.

In my opinion, Douady & Couder's (1992) effort to create a physical model of phyllotaxis represented a major advance in this field. They utilized tiny ferrofluid drops of equal volume floating on a circular dish of silicon oil to mimic leaf primordia being displaced off a shoot apex. The dish was exposed to a magnetic field that caused the drops to act as small magnetic dipoles capable of repelling each other with a force proportional to  $d^{-4}$ , where  $d$  is the distance between any two drops. The magnetic field was weakest at the centre and strongest at the edge so that the drops, once they were released onto the centre of the silicon oil, floated toward the edge. The spacing between the successive drops on the silicon oil was regulated by changing either the time interval between their release, or equivalently, the strength of the magnetic field, which affected their velocity toward the edge.

The results from this physical model are absolutely stunning (Fig. 9). If the drop release and/or movement rates were tuned so that only two successive drops were floating on the silicon oil at the same time, then the second drop was repelled by the previous drop, and thus they moved in opposite directions generating the equivalent of a distichous (1,1) phyllotaxis. Small increases in drop rate produced steady (1,2) and (3,5) patterns, as illustrated in Figure 10. Further increases resulted in the most robust drop patterns exhibiting even higher Fibonacci numbers in a step-

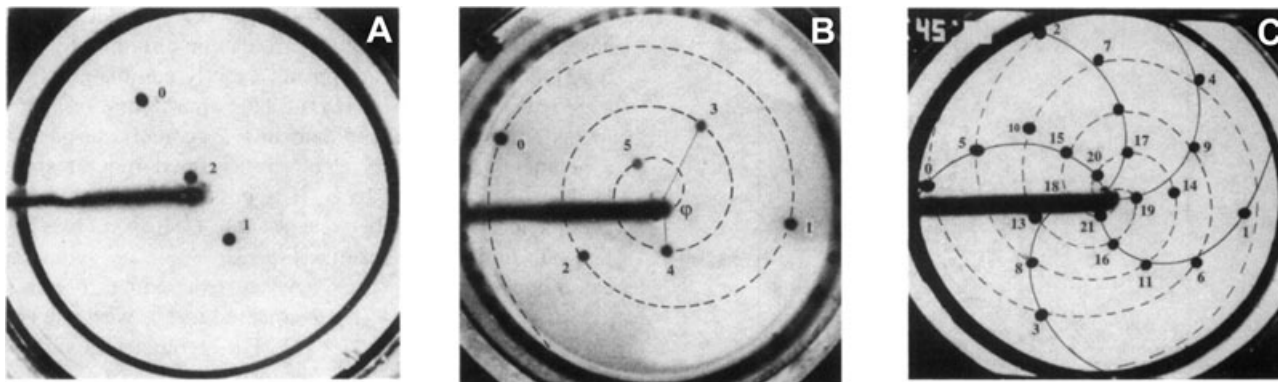


**Figure 9.** Three different Fibonacci patterns of ferrofluid drops floating on a dish of silicon oil and exposed to a magnetic field. The numbers show the sequence of the deposition of the drops, starting with drop 0 being the first drop released onto the centre of the dish. The drop patterns in panels A, B and C correspond to (1,1), (1,2), and (3,5) arrangements, respectively. Reproduced with permission from Douady & Couder (1992).

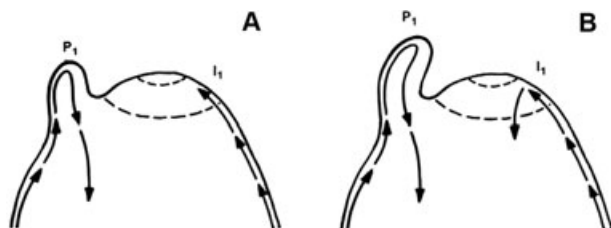


**Figure 10.** Hypothetical model for the role of polar auxin transport in phyllotaxis. A shoot apex is depicted in longitudinal section through the sites of  $P_1$  (the youngest visible primordium) and  $I_1$  (the next incipient primordium) at an early (panel A) and a later (panel B) stage of  $I_1$  initiation. Polar auxin flux is indicated with arrows. (A)  $P_1$  acts as an auxin sink to divert acropetal auxin flux, thereby preventing auxin accumulation above the  $P_1$  site but allowing auxin accumulation at the  $I_1$  site. (B) The auxin accumulation at the  $I_1$  site promotes the formation of a new primordium, which will, in turn, act as a new auxin sink. Reproduced with permission from Reinhardt *et al.* (2003).

wise fashion, with the maximum reaching the (13, 21) pattern. In essence, Douady & Couder (1992) managed to create spiral phyllotaxis on the lab bench.

Then they proceeded to link the fundamental process in their physical model, i.e. the mutual repulsion of magnetized ferrofluid drops, to the observations of inhibitory interactions among young leaf primordia on the shoot apex (Douady & Couder, 1996a, b, c). Computer simulations of their model were performed following either Hofmeister's (1868) rule that the incipient primordium arises in the largest space available at sequential intervals equal to the plastochron (Douady & Couder, 1996a) or Snow & Snow's (1952) modification that the primordium arises at the first

permissible site to achieve a certain minimum space (Douady & Couder, 1996b, c). In these simulations, the movements of the repelling elements, i.e. the model primordia, were restricted to the radial direction in order to make their behaviour resemble the displacement of real primordia off the shoot apex. These simulations were also able to display the spontaneous organization of model primordia into well-defined spiral phyllotaxes exhibiting the Fibonacci numbers characteristic of vegetative apices. Thus, their results are entirely consistent with earlier efforts to model spiral phyllotaxis on the basis of the action of a single diffusible inhibitor with a minimum threshold for permitting primordial initiation (Thornley, 1975; Mitchison, 1977; Veen & Lindenmayer, 1977) or the interaction between a local autocatalytic activator of primordial initiation and a long-range diffusible inhibitor (Meinhardt, 1984; Meinhardt, Koch & Bernasconi, 1998).

Several lines of experimental evidence suggest that the hormone auxin is a plausible candidate for this putative regulator of primordial positioning. In general, phyllotactic patterns are remarkably stable in response to experimental treatments; nevertheless, auxins and auxin regulatory compounds can profoundly alter vegetative phyllotaxis (for reviews, see Lyndon, 1998; Kuhlemeier & Reinhardt, 2001). For instance, Snow & Snow (1937) reported that auxin applied to the shoot apices of *Epilobium hirsutum* L. caused the origin of subsequent primordia to shift toward the site of auxin application, with the result that the phyllotaxis switched from the normal decussate to a spiral pattern. The polar auxin transport inhibitor triiodobenzoic acid converted the normal (2,3) phyllotaxis of *Chrysanthemum* seedlings into a distichous pattern (Schwabe, 1971). Other auxin reg-

ulatory compounds were similarly able to mediate the switch from decussate to spiral patterns on *Epilobium hirsutum* apices (Meicenheimer, 1981). In tomato apices, polar auxin transport inhibitors suppressed the formation of new leaf primordia, but subsequent localized applications of exogenous auxin induced leaf initiation along the same radial line as the auxin applications (Reinhardt, Mandel & Kuhlemeier, 2000).

Finally, recent molecular genetic studies have lent compelling support to this concept that auxin is intimately involved in phyllotactic patterning. Using *Arabidopsis thaliana* (L.) Heynh. as their experimental plant, Reinhardt *et al.* (2003) confirmed that new primordia arose at the sites of exogenous auxin application on the leafless apices of mutant *pin1* plants deficient in the auxin efflux protein PIN1. PIN1 is preferentially localized in the apical sides of the cells in the outermost layers of the shoot apical meristem so that Reinhardt *et al.* (2003) deduced that auxin must move in these layers up toward the apical dome. Because existing primordia are apparently acting as auxin sinks, highest auxin concentrations accumulate at the sites furthest from these primordia, with the result that these localized auxin accumulations can then trigger the initiation of new primordia (Fig. 10). Insofar as the gaps between existing primordia are thus determining the future sites of primordial initiation, this model provides a satisfying explanation for reiterative features of phyllotactic patterning. However, other plant hormones are also implicated in phyllotactic patterning. For instance, Giulini, Wang & Jackson (2004) studied the *abphyl1* mutant of *Zea mays* L. that initiates its leaves in a decussate pattern in contrast to the wild-type distichous pattern. The altered phyllotaxis in this mutant is attributable to a loss-of-function mutation in a cytokinin-inducible response regulator that affects the expansion of the shoot apical meristem. An overview of recent progress in the genetic regulation of leaf initiation is presented in Fleming (2005).

### CONCLUDING REMARKS

The most important contribution of this paper is that it establishes a rigorous criterion for evaluating whether or not a given phyllotaxis can be considered to represent a Fibonacci pattern. In particular, this criterion specifies that the numbers used to characterize the pattern are not sufficient by themselves to confirm an underlying Fibonacci operation, but rather such confirmation depends on whether or not the transitions to different phyllotactic numbers follow a discernible Fibonacci formula. The evidence presented here documents that the whorled phyllotaxes of both foliage leaves and floral organs often coincidentally exhibit Fibonacci numbers, but these phyllotaxes do

not represent Fibonacci patterns. By contrast, spiral phyllotaxes display developmental transitions to different numbers in the Fibonacci sequence so that these phyllotaxes can be classified as being genuine Fibonacci patterns. Nevertheless, there is no compelling evidence to suggest that leaf primordia in spiral phyllotaxes are being positioned in accordance with a global geometric imperative for optimal packing.

This interpretation is significant in light of our earlier paper on the relationship between apical geometry and phyllotactic patterns in aquatic angiosperms (Kelly & Cooke, 2003). Angiosperm lineages have re-invaded the aquatic environment around 200 times (Cook, 1999), which has apparently resulted in aquatic angiosperms having the potential to express a greater range of phyllotactic patterns than their terrestrial relatives. It is significant that those aquatic angiosperms generating whorled phyllotaxes are always characterized by unusual protuberant apices that initiate their leaf primordia on the lateral axis below the apical dome. By contrast, almost all aquatic plants retaining alternate, i.e. spiral, phyllotaxes of their terrestrial ancestors develop their leaves on the apical dome; rice, the sole exception to this generalization, is more appropriately viewed as a whorl of one (Kelly & Cooke, 2003). It is conceivable that the aquatic plants exhibiting whorled phyllotaxis had independently and repeatedly evolved new mechanisms for specifying that particular phyllotactic pattern. However, it seems more reasonable to propose that the same underlying mechanism for phyllotactic patterning is acting in all aquatic angiosperms, but the positional constraints restricting leaf initiation to the apical dome are no longer operating in those aquatic plants with protuberant apices, with the result that they can now initiate leaf primordia in whorls arising on their lateral axes. In other words, the same mechanism is apparently acting to generate both whorled and spiral phyllotaxes, with the selection between these alternative patterns depending on the relative position of leaf initiation. It follows that the appearance of Fibonacci relationships in phyllotactic patterning should not be considered as a general rule for angiosperms, but rather as a special case solely applying to those plants capable of initiating leaf primordia on their apical domes.

Another unifying principle governing phyllotactic patterns of seed plant shoots is that the positions of most, if not all, organs regardless of morphological identity are probably specified by one common mechanism or several related mechanisms associated with the initiation of leaves and other homologous lateral organs. Such mechanisms may also control the arrangements of other prominent structures such as ovuleriferous scales and disc flowers, because these structures arise in the axils of subtending bracts,

which are certainly homologous to leaves. However, although related mechanisms for phyllotactic patterning may be operating throughout the seed plants, it must be appreciated that leaves have independently evolved in several other lineages, including leafy liverworts, mosses and lycophytes (Cronk, 2001; Friedman, Moore & Purugganan, 2004). Thus, there is no *a priori* reason to believe that a universal mechanism for positioning all types of analogous leaves is operating in all land plant lineages.

Lastly, the common mechanism underlying phyllotactic patterns of seed plants, as is the case with other physical and biological patterns (e.g. Goodwin, 1994; Ball, 1999; Stewart, 2001), appears to involve the interaction of mathematical rules, generating process, and overall geometry. In particular, it seems quite plausible that the mathematical rules for phyllotaxis arise from local inhibitory interactions among existing primordia (Hofmeister, 1868; Snow & Snow, 1952; Douady & Couder, 1992). These interactions are apparently mediated by the expression of specific genes whose products regulate growth hormones (Kuhlemeier & Reinhardt, 2001; Reinhardt *et al.*, 2003) operating within the physical constraints imposed by shoot apical geometry (Kelly & Cooke, 2003). This interpretation will be evaluated in the next paper in this series.

#### NOTE ADDED IN PROOF

In larch somatic embryos, the number of cotyledons arranged in whorled phyllotaxis is directly correlated with apical diameter, which is consistent with other reports on whorled phyllotaxis presented in this paper. (Harrison LG, von Aderkas P. 2004. Spatially quantitative control of the number of cotyledons in a clonal population of somatic embryos of hybrid larch *Larix x leptoeuropaea*. *Annals of Botany* **93**: 423–433.) Confocal imaging of green fluorescent protein reporter genes is now being used to visualize the relationships among auxin transport dynamics, localized gene expression and morphogenetic processes occurring in shoot apical meristems (Heisler MG, Ohno C, Das P, Sieber P, Reddy GV, Long JA, Meyerowitz EM. 2005. Patterns of auxin transport and gene expression during primordium development revealed by live imaging of the *Arabidopsis* inflorescence meristem. *Current Biology* **15**: 1899–1911.)

#### ACKNOWLEDGEMENTS

This paper is dedicated to my friend Don Kaplan on the occasion of his retirement from the University of California, Berkeley. I thank Wanda Kelly (University of Maryland), Donald Kaplan (University of California, Berkeley), Leor Weinberger (Princeton Univer-

sity) and Peter Endress (University of Zurich) for their encouragement, assistance and criticism.

#### REFERENCES

- Adler I. 1974. A model of contact pressure in phyllotaxis. *Journal of Theoretical Biology* **45**: 1–79.
- Ball P. 1999. *The self-made tapestry: pattern formation in nature*. Oxford: Oxford University Press.
- Bierhorst DW. 1959. Symmetry in *Equisetum*. *American Journal of Botany* **46**: 170–179.
- Britton J. 2003. *Fibonacci numbers in nature*. <http://britton.disted.camosun.bc.ca/fibslide/jbfibslide.htm>
- Burt BL. 1978. Aspects of diversification in the capitulum. In: Heywood VH, Harborne JB, Turner BL, eds. *The biology and chemistry of the Compositae*, Vol. 1. London: Academic Press, 41–59.
- Church AH. 1920. *On the interpretation of phenomena of phyllotaxis*. London: Oxford University Press.
- Clark SE, Running MP, Meyerowitz EM. 1993. CLAVATA1, a regulator of meristem and flower development in *Arabidopsis*. *Development* **119**: 397–418.
- Clark SE, Running MP, Meyerowitz EM. 1995. CLAVATA3 is a regulator of shoot and floral meristem development affecting the same processes as CLAVATA1. *Development* **121**: 2057–2067.
- Coen ES, Meyerowitz EM. 1991. The war of the whorls: genetic interactions controlling flower development. *Nature* **353**: 31–37.
- Cook CDK. 1999. The number and kinds of embryo-bearing plants which became aquatic: a survey. *Perspectives in Plant Ecology, Evolution and Systematics* **2**: 79–102.
- Coxeter HSM. 1953. The golden section, phyllotaxis, and Wythoff's game. *Scripta Mathematica* **19**: 135–143.
- Cronk QCB. 2001. Plant evolution and development in a post-genomic context. *Nature Reviews Genetics* **2**: 607–619.
- Douady S, Couder Y. 1992. Phyllotaxis as a physical self-organized growth process. *Physical Review Letters* **68**: 2098–2101.
- Douady S, Couder Y. 1996a. Phyllotaxis as a dynamical self-organizing process. Part I. The spiral modes resulting from time-periodic iterations. *Journal of Theoretical Biology* **178**: 255–274.
- Douady S, Couder Y. 1996b. Phyllotaxis as a dynamical self-organizing process. Part II. The spontaneous formation of a periodicity and the co-existence of spiral and whorled patterns. *Journal of Theoretical Biology* **178**: 275–294.
- Douady S, Couder Y. 1996c. Phyllotaxis as a dynamical self-organizing process. Part III. The simulation of the transient regimes of ontogeny. *Journal of Theoretical Biology* **178**: 295–312.
- Dunlap RA. 1997. *The golden ratio and Fibonacci numbers*. Singapore: World Scientific.
- Endress PK. 1987. Flora phyllotaxis and floral evolution. *Botanische Jahrbucher fur Systematik* **108**: 417–438.
- Erickson RO. 1973. Tubular packing of spheres in biological fine structures. *Science* **181**: 705–716.

- Fleming AJ. 2005.** Formation of primordia and phyllotaxy. *Current Opinion in Plant Biology* **8**: 53–58.
- Friedman WE, Moore RC, Purugganan MD. 2004.** Evolution of plant development. *American Journal of Botany* **91**: 1726–1741.
- Fujita T. 1938.** Statistische Untersuchung über die Zahl konjugierten Parastichen bei den schraubigen Organstellungen. *Botanical Magazine* **52**: 425–433.
- Garland TH. 1987.** *Fascinating Fibonacci: mystery and magic in numbers*. Palo Alto, CA: Dale Seymour Publications.
- Giulini A, Wang J, Jackson D. 2004.** Control of phyllotaxy by the cytokinin-inducible regulator homologue ABPHYLL1. *Nature* **430**: 1031–1034.
- Goethe JW von. 1790.** *Versuch die Metamorphose der Pflanzen Zu Erklären*. Gotha: Ettinger.
- Goodwin B. 1994.** *How the leopard changed its spots: the evolution of complexity*. New York: Charles Scribner's Sons.
- Green PB. 1999.** Expression of pattern in plants: combining molecular and calculus-based biophysical-based paradigms. *American Journal of Botany* **86**: 1059–1076.
- Griffith ME, da Silva Conceição A, Smyth DR. 1999.** PETAL LOSS gene regulates initiation and orientation of second whorl organs in the *Arabidopsis* flower. *Development* **126**: 5635–5644.
- Hofmeister W. 1868.** *Allgemeine Morphologie des Gewachse, Handbuch der Physiologischen Botanik*. Leipzig: Engelmann.
- Hoggatt VE Jr. 1969.** *Fibonacci and Lucas numbers*. Boston: Houghton Mifflin Company.
- Huntley HE. 1970.** *The divine proportion: a study in mathematical beauty*. New York: Dover Publications.
- van Iterson G. 1907.** *Mathematische und Mikroskopisch-Anatomische Studien Über Blattstellungen, Nebst Betrachtungen Über Den Schalenbau der Miliolinen*. Jena: Gustav-Fischer-Verlag.
- Jean RV. 1984.** *Mathematical approach to pattern and form in plant growth*. New York: Wiley-Interscience.
- Jean RV. 1994.** *Phyllotaxis: a systemic study in plant morphogenesis*. Cambridge: Cambridge University Press.
- Kappraff J. 2002.** *Beyond measure: a guided tour through nature, myth, and number*. Singapore: World Scientific.
- Kelly WJ, Cooke TJ. 2003.** Geometrical relationships specifying the phyllotactic patterns of aquatic plants. *American Journal of Botany* **90**: 1131–1143.
- King S, Beck F, Lüttge U. 2004.** On the mystery of the golden angle in phyllotaxis. *Plant, Cell and Environment* **27**: 685–695.
- Knott R. 2004.** *The Fibonacci numbers and the golden section in nature – I*. <http://www.mcs.surrey.ac.uk/Personal/R.Knott/Fibonacci/fibnat.html>
- Koshy T. 2001.** *Fibonacci and Lucas numbers with applications*. New York: John Wiley & Sons.
- Kuhlemeier C, Reinhardt D. 2001.** Auxin and phyllotaxis. *Trends in Plant Science* **6**: 187–189.
- Laux T, Mayer KF, Berger J, Jurgens G. 1996.** The WUSCHEL gene is required for shoot and floral meristem integrity in *Arabidopsis*. *Development* **122**: 87–96.
- Leigh EG Jr. 1972.** The golden section and spiral leaf-arrangement. *Transactions of the Connecticut Academy of Arts and Sciences* **44**: 163–176.
- Leyser HMO, Furner IJ. 1992.** Characterization of three shoot apical meristem mutants of *Arabidopsis thaliana*. *Development* **116**: 397–403.
- Livio M. 2002.** *The golden ratio: the story of phi, the world's most astonishing number*. New York: Broadway Books.
- Lyndon RF. 1998.** *The shoot apical meristem: its growth and development*. Cambridge: Cambridge University Press.
- Mackay AL. 1998.** Prologue by a crystallographer: phyllotaxis. In: Jean RV, Barabé D, eds. *Symmetry in plants*. Singapore: World Scientific, xxxv–xxxix.
- Maksymowych R, Erickson RO. 1977.** Phyllotactic change induced by gibberellic acid in *Xanthium* shoot apices. *American Journal of Botany* **64**: 33–44.
- McCully ME, Dale HM. 1961.** Variations in leaf number in *Hippuris*: a study of whorled phyllotaxis. *Canadian Journal of Botany* **39**: 611–625.
- Meicenheimer RD. 1981.** Changes in *Epilobium* phyllotaxy induced by N-1-naphthylphthalamic acid and  $\alpha$ -4-chlorophenoxyisobutyric acid. *American Journal of Botany* **68**: 1139–1154.
- Meinhardt H. 1984.** Models of pattern formation and their application to plant development. In: Barlow PW, Carr DJ, eds. *Positional controls in plant development*. Cambridge: Cambridge University Press, 1–32.
- Meinhardt H, Koch A-J, Bernasconi G. 1998.** Models of pattern formation as applied to plant development. In: Jean RV, Barabé D, eds. *Symmetry in plants*. Singapore: World Scientific, 723–758.
- Mitchison GH. 1977.** Phyllotaxis and the Fibonacci series. *Science* **196**: 270–275.
- Niklas KJ. 1988.** The role of phyllotactic pattern as a 'development constraint' on the interception of light by leaf surfaces. *Evolution* **42**: 1–16.
- Niklas KJ. 1998.** Light harvesting 'fitness landscapes' for vertical shoots with different phyllotactic patterns. In: Jean RV, Barabé D, eds. *Symmetry in plants*. Singapore: World Scientific, 759–773.
- Palmer JH. 1998.** The physiological basis of pattern generation in the sunflower. In: Jean RV, Barabé D, eds. *Symmetry in plants*. Singapore: World Scientific, 145–169.
- Prusinkiewicz P, Lindenmayer A. 1990.** *The algorithmic beauty of plants*. New York: Springer.
- Reinhardt D, Mandel T, Kuhlemeier C. 2000.** Auxin regulates the initiation and radial position of plant lateral organs. *Plant Cell* **12**: 507–518.
- Reinhardt D, Pesce E-R, Stieger P, Mandel T, Baltensperger K, Bennett M, Traas J, Friml J, Kuhlemeier C. 2003.** Regulation of phyllotaxis by polar auxin transport. *Nature* **426**: 255–260.
- Richards FJ. 1948.** The geometry of phyllotaxis and its origin. In: Danielli JF, Brown R, eds. *Growth in relation to differentiation and morphogenesis, Symposia of the Society for Experimental Biology, Number 2*. Cambridge: Cambridge University Press, 217–245.
- Richards FJ. 1951.** Phyllotaxis: its quantitative expression and relation to growth in the apex. *Philosophical Transactions of the Royal Society of London, Series B* **235**: 509–564.
- Ridley JN. 1982a.** Computer simulation of contact pressure in capitula. *Journal of Theoretical Biology* **95**: 1–24.

**Ridley JN. 1982b.** Packing efficiency in sunflower heads. *Mathematical Biosciences* **58**: 129–139.

**Rivier N, Ocelli R, Pantaloni J, Lissowski A. 1984.** Structure of Benard convection cells, phyllotaxis and crystallography in cylindrical symmetry. *Journal de Physique* **45**: 49–63.

**Running MP, Meyerowitz EM. 1996.** Mutations in the PERIANTHIA gene of *Arabidopsis* specifically alter floral organ number and initiation pattern. *Development* **122**: 1261–1269.

**Schooling W. 1914.** The  $\Phi$  progression. In: Cook TA, ed. *The curves of life*. London: Constance, 441–447.

**Schwabe WW. 1971.** Chemical modification of phyllotaxis and its implications. In: Davies DD, Balls M, eds. *Control mechanisms of growth and differentiation, Symposia of the Society for Experimental Biology, Number 25*. Cambridge: Cambridge University Press, 301–322.

**Selvan AM. 1998.** Quasicrystalline pattern formation in fluid substrates and phyllotaxis. In: Jean RV, Barabé D, eds. *Symmetry in plants*. Singapore: World Scientific, pp. 795–809.

**Sloane NJA. 2004.** *The on-line encyclopedia of integer sequences*. <http://www.research.att.com/~njas/sequences>

**Snow M, Snow R. 1952.** Minimum areas and leaf determination. *Proceedings of the Royal Society of London B* **139**: 545–566.

**Snow M, Snow R. 1937.** Auxin and leaf formation. *New Phytologist* **36**: 1–18.

**Stewart I. 2001.** *What shape is a snowflake?* New York: W.H. Freeman.

**TAIR. 2004.** *The Arabidopsis Information Resource database*. <http://www.arabidopsis.org>

**Thompson D'AW. 1942.** *On growth and form*, 2nd edn. Cambridge: Cambridge University Press.

**Thornley JHM. 1975.** Phyllotaxis I: a mechanistic model. *Annals of Botany* **39**: 491–507.

**Tucker SC. 1961.** Phyllotaxis and vascular organization of the carpels in *Michelia fuscata*. *American Journal of Botany* **48**: 60–71.

**Vajda S. 1989.** *Fibonacci and Lucas numbers, and the golden section: theory and applications*. New York: Halsted Press.

**Veen AH, Lindenmayer A. 1977.** Diffusion mechanism for phyllotaxis: theoretical physico-chemical and computer study. *Plant Physiology* **60**: 127–139.

**Vogel H. 1979.** A better way to construct a sunflower head. *Mathematical Biosciences* **44**: 179–189.

**Vorobyov NN. 1963.** *The Fibonacci numbers*. Boston: D. C. Heath.

**Williams RF. 1975.** *The shoot apex and leaf growth: a study in quantitative biology*. Cambridge: Cambridge University Press.

**Wright C. 1873.** On the uses and origin of the arrangements of leaves in plants. *Memoirs of the American Academy of Arts and Sciences* **9**: 379–415.

APPENDIX

The alert reader will have noticed that the reciprocal  $1/\phi$  (or  $\phi^{-1}$ ) is numerically related to  $\phi$  as

**Table A1.** Numerical relationships between the geometric progressions of  $\phi$  (the so-called golden progressions) and the equivalent values expressed in terms of additive Fibonacci sequences. These relationships are generalized as a Fibonacci rule in the form of  $\phi^{n-2} + \phi^{n-1} = \phi^n$

Positive geometric progression		Negative geometric progression	
Powers of $\phi$	Equivalent values	Powers of $\phi$	Equivalent values
$\phi^0$	1	$\phi^0$	1
$\phi^1$	$1\phi$	$\phi^{-1}$	$1\phi - 1$
$\phi^2$	$1\phi + 1$	$\phi^{-2}$	$-1\phi + 2$
$\phi^3$	$2\phi + 1$	$\phi^{-3}$	$2\phi - 3$
$\phi^4$	$3\phi + 2$	$\phi^{-4}$	$-3\phi + 5$
$\phi^5$	$5\phi + 3$	$\phi^{-5}$	$5\phi - 8$
$\phi^6$	$8\phi + 5$	$\phi^{-6}$	$-8\phi + 13$
$\phi^7$	$13\phi + 8$	$\phi^{-7}$	$13\phi - 21$

$$\phi^{-1} = 0.6180339887... = \phi - 1.$$

It turns out that  $\phi^2$  is also numerically related to  $\phi$  as

$$\phi^2 = 2.6180339887... = \phi + 1.$$

Indeed,  $\phi$  displays almost mystical numerical properties. For instance, further calculations of the powers of  $\phi$  show that they exhibit a Fibonacci relationship to each other (Schooling, 1914; Huntley, 1970; Dunlap, 1997; Kappraff, 2002). In particular, Table A1 shows that the golden geometric progression of

$$\phi^1, \phi^2, \phi^3, \phi^4, \phi^5 \dots$$

corresponds to the additive sequence of

$$1\phi + 0, 1\phi + 1, 2\phi + 1, 3\phi + 2, 5\phi + 3, \dots, \text{ respectively.}$$

This relationship can be generalized as a Fibonacci rule in the form of

$$\phi^{n-2} + \phi^{n-1} = \phi^n.$$

The negative golden geometric progression exhibits the same mathematical properties except that it is an oscillating sequence, with the minus sign switching back and forth between the two terms. Thus, this negative geometric progression of

$$\phi^{-1}, \phi^{-2}, \phi^{-3}, \phi^{-4}, \phi^{-5} \dots$$

is equivalent to the additive sequence of

$$1\phi - 1, -1\phi + 2, 2\phi - 3, -3\phi + 5, 5\phi - 8, \dots, \text{ respectively.}$$

Rearranging the above Fibonacci rule indicates the higher negative power of  $\phi^{n-2}$  is related to the previous two lower powers of  $\phi^n$  and  $\phi^{n-1}$  by

$$\phi^n - \phi^{n-1} = \phi^{n-2}.$$

Similar mathematical relationships are observed between primary fractional Fibonacci sequences and their limits (Table A2). For example, the primary fractional sequence starting with  $2/1$ ,  $3/2$  and  $5/3$  has a limit of  $\phi$ . It turns out that the fractional sequence starting with  $3/1$ ,  $5/2$  and  $8/3$  has a limit of  $\phi^2$ , the next one starting with  $5/1$ ,  $8/2$ , and  $13/3$  has a limit of  $\phi^3$ , etc. An analogous pattern is observed with the corresponding reciprocal primary fractional sequences and their limits calculated as negative powers of  $\phi$ . These relationships can be summarized as: the limit of any given primary fractional sequence is equal to  $\phi^{a-b}$ , where  $a$  and  $b$  refer to the respective positions in the original primary sequence of the two numbers ( $x_a/x_b$ ) used to start the fractional sequence under study.

It should be clear from this brief discussion why  $\phi$ , and related Fibonacci sequences, are entrancing to even those of us who are virtually untrained in formal mathematics.

**Table A2.** Some characteristics of primary fractional Fibonacci sequences with an initial term of  $x_a/x_b$ , where  $x_a$  and  $x_b$  are the  $a$ th and  $b$ th terms in the primary Fibonacci sequence (1, 2, 3, 5, 8, ...). The limit of each fractional sequence is calculated as  $\phi^{a-b}$

Sequence	Initial term	Limit
$1/2, 2/3, 3/5, \dots$	$x_1/x_2$	$\phi^{-1}$
$1/3, 2/5, 3/8, \dots$	$x_1/x_3$	$\phi^{-2}$
$1/5, 2/8, 3/13, \dots$	$x_1/x_4$	$\phi^{-3}$
$1/8, 2/13, 3/21, \dots$	$x_1/x_5$	$\phi^{-4}$
$1/13, 2/21, 3/34, \dots$	$x_1/x_6$	$\phi^{-5}$
$2/1, 3/2, 5/3, \dots$	$x_2/x_1$	$\phi$
$3/1, 5/2, 8/3, \dots$	$x_3/x_1$	$\phi^2$
$5/1, 8/2, 13/3, \dots$	$x_4/x_1$	$\phi^3$
$8/1, 13/2, 21/3, \dots$	$x_5/x_1$	$\phi^4$
$13/1, 21/2, 34/3, \dots$	$x_6/x_1$	$\phi^5$